Deletions of Helices 2 and 3 of Human ApoA-I Are Associated with Severe Dyslipidemia following Adenovirus-Mediated Gene Transfer in ApoA-I-Deficient Mice†

Angeliki Chroni, Horng-Yuan Kan, Adelina Shkodrani, Tong Liu, and Vassilis I. Zannis*

Section of Molecular Genetics, Whitaker Cardiovascular Institute, Departments of Medicine and Biochemistry, Boston University School of Medicine, Boston, Massachusetts 02118

Received September 16, 2004; Revised Manuscript Received November 9, 2004

ABSTRACT: The objective of this study was to determine the effect of two amino-terminal apolipoprotein A-I (apoA-I) deletions on high-density lipoprotein (HDL) biosynthesis and lipid homeostasis. Adenovirus-mediated gene transfer showed that the apoA-I[Δ(89−99)] deletion mutant caused hypercholesterolemia, characterized by increased plasma cholesterol and phospholipids, that were distributed in the very low density/intermediate density/low-density lipoprotein (VLDL/IDL/LDL) region, and normal triglycerides. The capacity of the mutant protein to promote ATP-binding cassette transporter A1- (ABCA1-) mediated cholesterol efflux and to activate lecithin:cholesterol acyltranserase (LCAT) was approximately 70−80% of the wild-type (WT) control. The phospholipid transfer protein (PLTP) activity of plasma containing the apoA-I[Δ(89−99)] mutant was decreased to 32% of the WT control. Similar analysis showed that the apoA-I[Δ(62−78)] deletion mutant in apoA-I-deficient mice caused combined hyperlipidemia characterized by increased triglycerides, cholesterol, and phospholipids in the VLDL/IDL region. There was enrichment of the VLDL/IDL with mutant apoA-I that resulted in reduction of in vitro lipolysis. The capacity of this mutant to promote ABCA1-mediated cholesterol efflux was normal, and the capacity to activate LCAT in vitro was reduced by 53%. The WT apoA-I and the apoA-I[Δ(62−78)] mutant formed spherical HDL particles, whereas the apoA-I[Δ(89−99)] mutant formed discoidal HDL particles. We conclude that alterations in apoA-I not only may have adverse effects on HDL biosynthesis but also may promote dyslipidemia due to interference of the apoA-I mutants on the overall cholesterol and triglycerides homeostasis.

Apolipoprotein A-I (apoA-I)[1] is the major protein constituent of high-density lipoproteins (HDL) and plays a crucial role in the biogenesis, structure, function, and plasma concentration of HDL (*1*−*5*). The biogenesis and catabolism of HDL can be considered as a complex pathway that involves several proteins (*5*). In the early steps of this pathway, apolipoprotein (apoA-I) is secreted mostly lipid-free by the liver and acquires phospholipid and cholesterol via its interactions with the ATP-binding cassette A1 (ABCA1) lipid transporter. Through a series of intermediate steps that are poorly understood, apoA-I is gradually lipidated and proceeds to form discoidal particles, which are converted to spherical particles by the action of lecithin:cholesterol acyltransferase (LCAT). Both discoidal and spherical HDL particles interact functionally with the HDL receptor scavenger receptor class B type I (SR-BI). The late steps of the HDL pathway involve the transfer of cholesteryl esters to VLDL/LDL for eventual catabolism by the LDL receptor, the hydrolysis of phospholipids and residual triglycerides by the various lipases (lipoprotein lipase, hepatic lipase, and endothelial lipase), and the transfer of phospholipids from VLDL/LDL to HDL by the action of phospholipid transfer protein.

We have recently performed functional in vitro studies of apoA-I, as well as gene transfer of apoA-I mutants in apoA-I-deficient (apoA-$I^{-/-}$) mice, to ascertain the physiological interactions of apoA-I with other proteins of the HDL pathway and the role of apoA-I in the biogenesis and the functions of HDL. The early studies showed that mutations that prevent binding of apoA-I to phospholipid and HDL in vitro resulted in low apoA-I and HDL levels in vivo, following gene transfer of mutant apoA-I forms in apoA-$I^{-/-}$ mice, due to defective maturation of discoidal to spherical HDL particles (*6*). In subsequent studies we probed the interactions between ATP-binding cassette transporter

† This work was supported by National Institutes of Health Grants HL-33952 and HL-48739 and by KOS Pharmaceuticals, Miami, FL.

* To whom correspondence should be addressed: Tel 617-638-5085; fax 617-638-5141; e-mail:vzannis@bu.edu.

[1] Abbreviations: ABCA1, ATP-binding cassette transporter A1; apoA-I, apolipoprotein A-I; apoA-$I^{-/-}$ mice, apoA-I-deficient mice; BSA, bovine serum albumin; CETP, cholesteryl ester transfer protein; DMEM, Dulbecco's modified Eagle's medium; DMPC, dimyristoyl-L-α-phosphatidylcholine; DPPC, dipalmitoyl-L-α-phosphatidylcholine; EDTA, ethylenediaminetetraacetic acid; ELISA, enzyme-linked immunosorbent assay; EM, electron microscopy; FBS, fetal bovine serum; HDL, high-density lipoprotein; HEK cells, human embryonic kidney cells; HL, hepatic lipase; IDL, intermediate-density lipoprotein; LCAT, lecithin:cholesterol acyltransferase; LDL, low-density lipoprotein; LPL, lipoprotein lipase; NEFA, nonesterified fatty acids; PBS, phosphate-buffered saline; PLTP, phospholipid transfer protein; POPC, β-oleoyl-γ-palmitoyl-L-α-phosphatidylcholine; rTEV protease, recombinant tobacco etched viral protease; VLDL, very low density lipoprotein; WT, wild type.

10.1021/bi047998l CCC: $30.25
Published on Web 02/18/2005

A1 (ABCA1) and apoA-I in relation to the biogenesis of HDL (*2*, *5*, *7*). These studies showed that residues 220−231, as well as the central helices of apoA-I, participate in ABCA1-mediated lipid efflux and HDL biogenesis (*2*, *5*, *7*). In the present study we have analyzed the in vivo phenotypes of two interesting apoA-I mutations and have correlated the observed phenotypes with known interactions of apoA-I with other proteins of the HDL pathway. Here we show that mutations in apoA-I not only may affect the HDL metabolism but also may have adverse effects on the overall cholesterol and triglycerides homeostasis. An apoA-I[Δ(89−99)] deletion mutant generated a phenotype that has not been encountered previously. This deletion affected the maturation of HDL, inhibited the activity of phospholipid transfer protein (PLTP), and promoted the accumulation of abnormal lipoprotein particles in the VLDL/IDL/LDL region. The apoA-I[Δ(62−78)] deletion resulted in a severe hypertriglyceridemic phenotype characterized by accumulation of apoA-I containing triglycerides-rich remnants in the VLDL/IDL region. This phenotype is similar to that produced by substitutions of Glu110 and Glu111of apoA-I by Ala (*8*), indicating that different structural mutations in apoA-I may induce hypertriglyceridemia.

EXPERIMENTAL PROCEDURES

Materials. Materials not mentioned in the Experimental Procedures have been obtained from sources described previously (*8*).

Generation of Adenoviruses and Baculoviruses Expressing Wild-Type and Mutant ApoA-I Forms. The construction of recombinant adenoviruses carrying the genomic sequence for WT proapoA-I has been described before (*6*). The adenoviruses expressing apoA-I[Δ(62−78)] and apoA-I[Δ(89−99)] were generated in a similar way. For apoA-I[Δ(62−78)] the sequence of the human apoA-I gene was amplified and mutagenized by polymerase chain reaction, using a set of specific mutagenic primers D(62−78)F (5′-C TCC ACC TTC AGC AAG CTG CGC ACA GAG GGC CTG AGG CAG GAG 3′) and D(62−78)R (5′-CTC CTG CCT CAG GCC CTC TGT GCG CAG CTT GCT GAA GGT GGA G-3′) containing the deletion of interest and a set of flanking universal primers (PCA13FONT, 5′-GGG GAT CAG TCT TCG AGT CGA CAA GCT TGA-3′; PCA13END, 5′-GCA ATA AAC AAG TTG CTC GAT GGA TCC CTC-3′) containing the restriction sites *Sal*I and *Bam*HI. The pCA13AIgN vector, which contains a *Sal*I site before exon 1 and a *Sal*I followed by a *Bam*HI site in the 3′-end of the apoA-I gene, was used as a template in the amplification reactions (*6*). The DNA fragment containing the mutation of interest was digested with *Sal*I and subcloned into the *Sal*I sites of the pCA13 vector (MicroBix Biosystems, Canada). The correct orientation of the apoA-I gene in the pCA13 vector was determined by *Hin*dIII digestion. For apoA-I[Δ(89−99)] the fourth exon of the human apoA-I gene was amplified and mutagenized by polymerase chain reaction, using a set of specific mutagenic primers AIMIII1-5 (5′-CAG GAG ATG AGC AAG TAC CTG GAC GAC TTC-3′) and AIMIII1-3 (5′-GAA GTC GTC CAG GTA CTT GCT CAT CTC CTG-3′) containing the mutation of interest and a set of flanking universal primers (AINOTF, 5′ CCT CCG CGG ACA GGC GGC CGC CAG GG 3′; AISALR, 5′ A CAT GTC GAC CCC CTT TCA GGG CAC CTG GCC TTG 3′) containing the restriction sites *Not*I and *Sal*I. The pCA13AIgN vector, which contains a *Not*I site in intron 3 and a *Xho*I site in the 3′-end of the apoA-I gene, was used as a template in the amplification reactions (*6*). The DNA fragment containing the mutation of interest was digested with *Not*I and *Sal*I and subcloned into the *Not*I and *Xho*I sites of the pCA13AIgN vector, thus replacing the WT with the mutated exon 4 sequence. The pCA13-A-I plasmids containing the 62−78 or the 89−99 deletion along with a helper PJM17 adenovirus plasmid were used to generate recombinant adenoviruses as described previously (*6*).

The expression and purification of recombinant WT apoA-I or the apoA-I[Δ(61−78)] and apoA-I[Δ(89−99)] deletion mutants in the baculovirus expression system was performed as described previously (*7*).

Animal Studies, Plasma Lipids, ApoA-I, and ApoA-I mRNA Level Analyses. ApoA-I$^{-/-}$ (apoA1^{tm1Unc}) C57BL/6J mice (*9*) were purchased from Jackson Laboratories (Bar Harbor, ME). The mice were maintained on a 12-h light/dark cycle and standard rodent chow. All procedures performed on the mice were in accordance with National Institutes of Health and institutional guidelines. ApoA-I$^{-/-}$ mice, 6−8 weeks of age, were injected via the tail vein with 1×10^9 plaque-forming units (pfu) of recombinant adenovirus per animal and the animals were sacrificed 4 days postinjection following a 4-h fast.

The concentration of total cholesterol, free cholesterol, phospholipids, and triglycerides of plasma drawn 4 days postinfection was determined by use of the Cholesterol CII, Free Cholesterol C, and Phospholipids B reagents (Wako Chemicals USA, Inc.) and Infinity triglycerides reagent (ThermoDMA), respectively, according to the manufacturer's instructions. The concentration of cholesteryl esters was determined by subtracting the concentration of free cholesterol from the concentration of total cholesterol. Plasma apoA-I levels and hepatic human apoA-I mRNA levels were determined as described (*2*, *4*).

For FPLC analysis of plasma, 17 μL of plasma obtained from mice infected with adenovirus-expressing WT or mutant apoA-I forms was loaded onto a Sepharose 6 PC column (Amersham Biosciences) in a SMART micro FPLC system (Amersham Biosciences) and eluted with PBS. A total of 25 fractions of 50 μL volume each were collected for further analysis. The concentration of lipids in the FPLC fractions was determined as described above.

Fractionation of Plasma by Density Gradient Ultracentrifugation and Electron Microscopy Analysis of the ApoA-I-Containing Fractions. For this analysis, 300 μL of plasma obtained from adenovirus-infected mice was diluted with saline to a total volume of 0.5 mL. The mixture was adjusted to a density of 1.23 g/mL with KBr and overlaid with 1 mL of KBr solution of $d = 1.21$ g/mL, 2.5 mL of KBr solution of $d = 1.063$ g/mL, 0.5 mL of KBr solution of $d = 1.019$ g/mL, and 0.5 mL of normal saline. The mixture was centrifuged for 22 h in an SW55 rotor at 30 000 rpm. Following ultracentrifugation, 0.5 mL fractions were collected from the top and analyzed as described (*2*). The first density gradient ultracentrifugation fraction obtained from the plasma of mice expressing the apoA-I[Δ(62−78)] mutant was further analyzed by SDS−PAGE and Western blotting. The nitrocellulose membranes were probed with goat polyclonal anti-mouse apoB, apoE, and apoCII antibodies (Santa

Table 1: Comparison of Plasma Cholesterol, Triglyceride, Phospholipid, ApoA-I, and Hepatic mRNA Levels of ApoA-I$^{-/-}$ Mice[a]

	cholesterol (mg/dL)	triglycerides (mg/dL)	phospholipids (mg/dL)	apoA-I (mg/dL)	relative apoA-I mRNA (%)
WT apoA-I	110 ± 30	104 ± 20	294 ± 57	479 ± 168	100
apoA-I[Δ(89-99)]	355 ± 38	82 ± 16	438 ± 40	146 ± 5	128 ± 25
apoA-I[Δ(62-78)]	220 ± 16	986 ± 289	707 ± 20	265 ± 36	130 ± 5
apoA-I$^{-/-}$	31 ± 9	33 ± 10	92 ± 15		

[a] Values are means ± SD ($n = 3-7$) and were measured prior to or 4 days postinfection with recombinant adenoviruses expressing WT apoA-I or apoA-I[Δ(62−78)] and apoA-I[Δ(89−99)] mutants.

Cruz Biotechnology, Inc., Santa Cruz, CA) for detection of the corresponding proteins.

For electron microscopy analysis, the fractions that float in the HDL region were treated and photographed as described previously (*2*).

Nondenaturating Two-Dimensional Electrophoresis. The distribution of HDL subfractions in plasma was analyzed by two-dimensional electrophoresis as described (*10*) with some modifications. Briefly, in the first dimension, 1 μL of plasma sample was separated by electrophoresis at 4 °C in a 0.75% agarose gel with a 50 mM barbital buffer (pH 8.6; Sigma, St. Louis, MO) until the bromophenol blue marker had migrated 5.5 cm. Agarose gel strips containing the separated lipoproteins were then transferred to a 4−20% polyacrylamide gradient gel. Separation in the second dimension was performed at 90 V for 2−3 h at 4 °C. The separated proteins were transferred to a nitrocellulose membrane and apoA-I was detected by using a goat polyclonal anti-human apoA-I antibody (Chemicon International).

In Vitro Lipolysis of Triglycerides of the VLDL Plasma Fraction. Increasing triglycerides concentrations of the VLDL/IDL fraction (fraction 1) obtained from plasma of apoA-I-deficient mice expressing WT apoA-I and apoA-I[Δ(62−78)] mutant were used as substrate in lipolysis experiments. Aliquots of VLDL/IDL in a final volume of 40 μL were adjusted to 2% fatty acid-free BSA in 100 mM Tris-HCl, pH 8.5, and were incubated with 34 ng of lipoprotein lipase (LPL) (Sigma) for 15 min at 37 °C. The released free fatty acids were quantified by use of an enzymatic colorimetric reagent, NEFA C (Wako Chemicals, Germany). Background values were determined by omitting LPL for each substrate concentration. LPL activity is expressed as micromoles of nonesterified fatty acid released per hour per milligram of LPL. To calculate the apparent V_{max} and K_m, the rate of free fatty acid release was plotted versus the concentration of triglycerides. The data were fitted to Michaelis−Menten kinetics, using the Prism software (GraphPad Software, Inc.).

Assay of PLTP Activity. To prepare phosphatidylcholine (PC) liposomes (*11*), 10 μmol of egg PC, 1 μCi of [^{14}C]-DPPC (dipalmitoyl-L-α-phosphatidylcholine [*dipalmitoyl*-1-^{14}C]; 0.05 mCi/mL, specific activity 110 mCi/mmol; Perkin-Elmer Life Sciences, Inc.), and 20 nmol of butylated hydroxytoluene were dried under nitrogen. To the dried lipids was added 1 mL of 10 mM Tris-HC1 buffer, pH 7.4, containing 150 mM NaCl and 1 mM EDTA, and the mixture was sonicated for 3 × 5 min in an ice bath with the microtip of a sonifier. After centrifugation for 10 min at 15 000 rpm in a microfuge, the optically clear supernatant was used for PLTP assays.

The assay contained human HDL (125 μg of protein), liposomes (75 nmol of [^{14}C]PC-labeled liposomes), plasma sample (1 μL), and 10 mM Tris-HC1 buffer, pH 7.4, containing 150 mM NaC1 and 1 mM EDTA in a final volume of 200 μL (*12*). Tubes without sample were included in each run. The assays were performed at 37 °C in Eppendorf tubes with 30-min incubations. The reaction was stopped by the addition of 0.15 mL of 536 mM NaCl and 363 mM $MnC1_2$ (containing 52 units of heparin), yielding final concentrations of 230 mM NaC1, 156 mM $MnC1_2$, and 74 units of heparin/mL. The tubes were vortexed for 10 s and, after standing for 10 min at room temperature, centrifuged for 10 min at 15 000 rpm. The supernatant (0.3 mL) was used for radioactivity determinations. The results are expressed as nanomoles of phosphatidylcholine transferred from PC liposomes to HDL per hour per milliliter of plasma. The plasma sample volume and incubation time were chosen so that the phospholipid transfer remained in the linear range. The transfer of radioactive phospholipid during the 30-min incubation was less than 13% of the total vesicle radioactivity.

Lecithin:Cholesterol Acyltransferase Production, Purification, and Activation by WT and Mutant ApoA-I Forms. LCAT was purified (*8*, *13*, *14*) from the culture medium of human HTB13 cells infected with an adenovirus expressing the human LCAT cDNA (*15*), which was a generous gift of Dr. Santamarina-Fojo. For LCAT analysis, the reconstituted HDL (rHDL) particles used as substrate contained cholesterol + [^{14}C]cholesterol ([4-^{14}C]cholesterol; 0.04 mCi/mL, specific activity 45 mCi/mmol; Perkin-Elmer Life Sciences, Inc.), β-oleoyl-γ-palmitoyl-L-α-phosphatidylcholine (POPC), and apoA-I and were prepared by the sodium cholate dialysis method as described (*3*, *16*). The reactions were carried as described (*3*, *8*). The cholesterol esterification rate was expressed as nanomoles of cholesteryl ester formed per hour. To calculate the apparent V_{max} and K_m, the rate of cholesteryl ester formation was plotted versus the concentration of apoA-I. The data were fitted to Michaelis−Menten kinetics, by use of Prism software (GraphPad Software, Inc.).

RESULTS

Plasma Lipid, ApoA-I, and Hepatic ApoA-I mRNA Levels following Adenovirus Infection. Analysis of plasma apoA-I and hepatic apoA-I mRNA levels 4 days postinfection showed that apoA-I$^{-/-}$ mice infected with adenoviruses expressing WT apoA-I and apoA-I[Δ(89−99)] and apoA-I[Δ(62−78)] deletion mutants had high plasma apoA-I concentration (479, 146, and 265 mg/dL, respectively). These differences in plasma apoA-I levels may not reflect differences in apoA-I expression, since the relative amounts of apoA-I mRNA were comparable (Table 1). In addition, the

WT and the two apoA-I mutant forms were secreted with the same efficiency into the medium of HTB-13 cells following infection with adenoviruses expressing WT apoA-I and the two apoA-I mutants (data not shown). However, we cannot exclude the possibility of differences in translation efficiencies or in vivo secretion of the two apoA-I mutants. The cholesterol and triglyceride levels of mice expressing WT and the two mutant apoA-I forms did not correlate with the plasma apoA-I levels. Mice expressing the apoA-I[Δ(89−99)] mutant had increased plasma cholesterol and phospholipids levels and normal triglycerides levels, whereas mice expressing the apoA-I[Δ(62−78)] mutant had higher plasma cholesterol and phospholipids levels and displayed severe hypertriglyceridemia (Table 1).

FPLC Profiles of Plasma Isolated from Mice Infected with Adenoviruses Expressing WT and Two Mutant ApoA-I Forms. FPLC analysis of plasma from apoA-I$^{-/-}$ mice infected with recombinant adenoviruses expressing either WT or the two apoA-I mutant forms, 4 days postinfection, showed that in mice expressing the WT apoA-I, cholesterol and phospholipids were distributed predominantly in the HDL2 and HDL3 region. In mice expressing the apoA-I[Δ(89−99)] mutant, the majority of cholesterol and phospholipids was found in the VLDL to LDL region (Figure 1A,B). These mice had normal amounts of triglycerides that were distributed in the VLDL region (Figure 1C). In mice expressing the apoA-I[Δ(62−78)] mutant, approximately 65% of cholesterol and phospholipids were distributed in the VLDL, 26% in the HDL, and small amounts in the LDL region (Figure 1A,B). The triglycerides levels in mice expressing this apoA-I mutant were high and were distributed in the VLDL region (Figure 1C).

Plasma fractions obtained from FPLC were further analyzed for the content of free and esterified cholesterol. These analyses are shown in Figure 1D−F for WT apoA-I, apoA-I[Δ(89−99)], and apoA-I[Δ(62−78)], respectively. The ratio of CE/TC of the FPLC fractions 14−21 that correspond to the HDL region for mice expressing WT apoA-I and the two apoA-I mutants and for apoA-I$^{-/-}$ mice is shown in Figure 1G. Similar results were obtained by density gradient ultracentrifugation of plasma and are shown later in Figure 2B. As shown in Figure 1G, the CE/TC ratio of the HDL fraction obtained from mice infected with the apoA-I[Δ(89−99)] mutant is greatly reduced. Compared to WT apoA-I, the ratio CE/TC in the LDL fraction was also reduced (0.31 for apoA-I[Δ(89−99)] vs 0.60 for WT apoA-I (data not shown)). This indicates defective in vivo esterification of HDL and LDL cholesterol. Smaller decrease in CE/TC ratio of HDL is also observed in apoA-I$^{-/-}$ mice.

Effect of ApoA-I[Δ(89−99)] and ApoA-I[Δ(62−78)] Mutations on the Distribution of ApoA-I in Different Lipoproteins and Size and Shape of HDL. Analysis of the distribution of apoA-I following density gradient ultracentrifugation of plasma showed that WT apoA-I was predominantly distributed in the HDL2 and HDL3 region (Figure 2A). Consistent with the FPLC data, the peak concentration of apoA-I[Δ(89−99)] mutant was in the HDL2 region. In addition, higher concentrations of mutant apoA-I were distributed in the LDL region as compared to WT apoA-I. Similarly, the peak concentration of apoA-I[Δ(62−78)] mutant was in the HDL2 and HDL3 region. However a small fraction of apoA-I was found in the VLDL/IDL and LDL region (Figure 2A).

Analysis of the distribution of total cholesterol, cholesteryl ester, free cholesterol, triglycerides, and phospholipids following density gradient ultracentrifugation of plasma essentially confirmed the distribution of these lipids to different lipoprotein fractions, obtained by FPLC fractionation (data not shown). The CE/TC ratio was calculated in fractions 4−8, which correspond to the HDL region that contains all the WT apoA-I and the majority of the mutant apoA-I forms. This analysis showed that the CE/TC ratio was greatly reduced for mice expressing the apoA-I[Δ(89−99)] mutant and to a lesser extent for mice expressing the apoA-I[Δ(62−78)] mutant and apoA-I$^{-/-}$ mice (Figure 2B). The diminished CE/TC ratio supports defective in vivo esterification of cholesterol by LCAT.

Analysis by electron microscopy of the HDL fractions, obtained by density gradient ultracentrifugation, that contain the highest apoA-I concentration showed that the apoA-I[Δ(89−99)] mutant formed discoidal HDL particles (Figure 2D), whereas both WT and the apoA-I[Δ(62−78)] mutant formed spherical HDL particles (Figure 2C,E), and apoA-I$^{-/-}$ mice formed a small number of spherical particles (Figure 2F). The average size of spherical HDL particles that contained the apoA-I[Δ(62−78)] mutant was increased as compared to WT apoA-I. Two-dimensional gel electrophoresis of plasma showed that in the apoA-I[Δ(89−99)] mutant approximately 50% of HDL was found in the form of preβ1 particles and 50% as αHDL (Figure 2H), whereas both WT apoA-I and apoA-I[Δ(62−78)] mutant formed αHDL particles and small amounts of preβ1 particles (Figure 2G,I).

Diminished Hydrolysis of Triglycerides of VLDL/IDL Fraction Obtained from Mice Expressing ApoA-I[Δ(62−78)] Mutant. Analysis of the ability of purified LPL to promote lipolysis showed that triglycerides of VLDL/IDL fraction obtained from the plasma of mice infected with adenovirus expressing the apoA-I[Δ(62−78)] mutant was hydrolyzed less efficiently than triglycerides of VLDL/IDL fraction obtained from mice infected with the adenovirus expressing WT apoA-I. The reduced catalytic efficiency of the enzyme (V_{maxapp}/K_{mapp}) was mainly due to the reduction in the V_{maxapp} (Figure 3A).

Consistent with the decreased lipolysis of VLDL/IDL, analysis of the apolipoprotein composition of the VLDL/IDL fraction obtained from mice expressing WT apoA-I or apoA-I[Δ(62−78)] mutant showed that VLDL/IDL containing the mutant apoA-I form had increased apoB-48 and decreased apoCII levels (Figure 3B).

The rate of hepatic VLDL triglyceride secretion following injection of Triton WR1339 (*17*) in mice expressing WT and apoA-I[Δ(62−78)] mutant was similar (data not shown).

Functional Analyses of WT and the Two Mutant ApoA-I Forms: (i) Activation of LCAT. For the LCAT activation assay, the WT and mutant apoA-I forms used for the generation of rHDL particles were isolated in the baculovirus system as described previously (*7*). The LCAT activity was assayed as the rate of production of labeled cholesteryl esters from the rHDL particles. The apparent catalytic efficiency (V_{maxapp}/K_{mapp}) of the enzyme with rHDL particles containing apoA-I[Δ(89−99)] and apoA-I[Δ(61−78)] mutant forms was reduced approximately to 77% and 47% as compared to rHDL particles containing WT apoA-I. The apparent catalytic

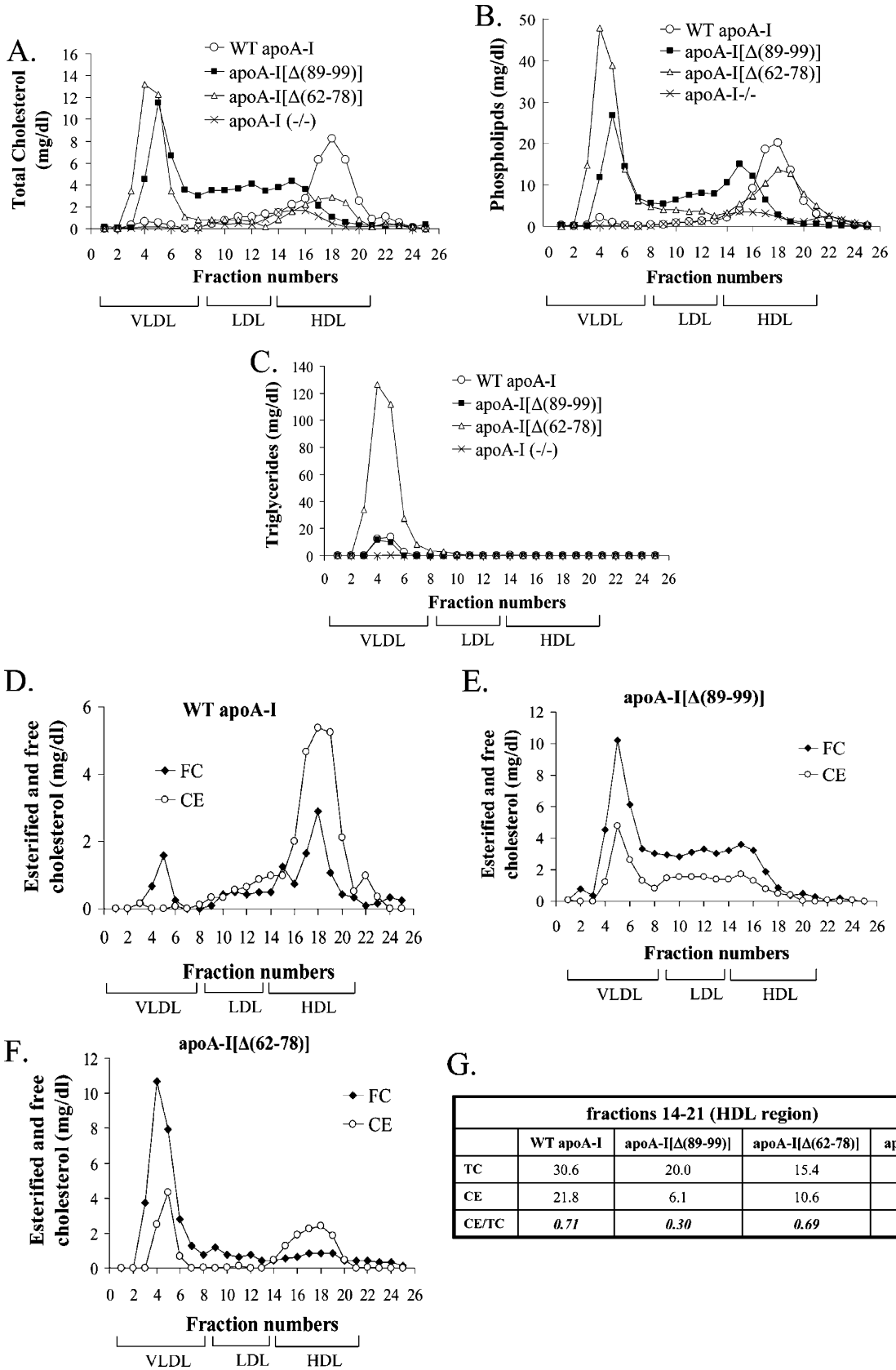

G.

fractions 14-21 (HDL region)				
	WT apoA-I	apoA-I[Δ(89-99)]	apoA-I[Δ(62-78)]	apoA-I$^{-/-}$
TC	30.6	20.0	15.4	6.5
CE	21.8	6.1	10.6	3.4
CE/TC	*0.71*	*0.30*	*0.69*	*0.52*

FIGURE 1: FPLC profiles of (A) total cholesterol, (B) phospholipids, (C) triglycerides, and (D−F) free cholesterol and cholesteryl esters in plasma of apoA-I$^{-/-}$ mice expressing WT apoA-I, apoA-I[Δ(89−99)] mutant, and apoA-I[Δ(62−78)] mutant. **(**G) Ratio of CE/TC levels of FPLC fractions 14−21, which correspond to the HDL region.

efficiency of rHDL particles containing apoA-I[Δ(89−99)] mutant with a His tag was 55% as compared to rHDL particles containing WT apoA-I (data not shown). The decrease in catalytic efficiency was accounted for by a reduction in V_{maxapp} of the enzymatic reaction with rHDL particles containing apoA-I[Δ(89−99)] mutant and an increase in K_{mapp} of the enzymatic reaction with rHDL particles containing apoA-I[Δ(61−78)] mutant (Figure 4A).

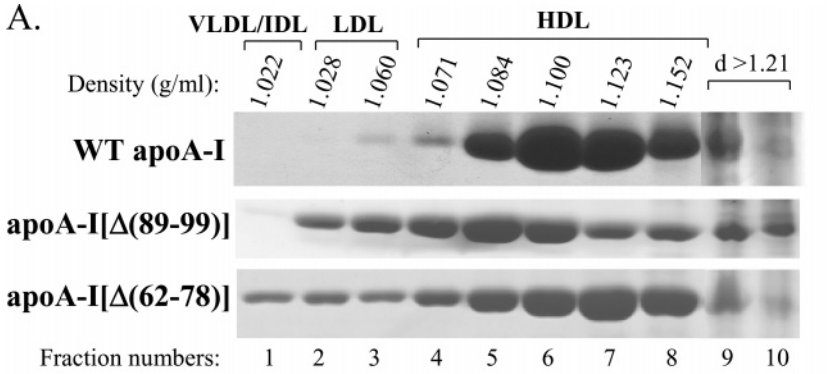

B.

fractions 4-8 (HDL region)				
	WT apoA-I	**apoA-I[Δ(89-99)]**	**apoA-I[Δ(62-78)]**	**apoA-I$^{-/-}$**
TC	34.3	72.1	49.3	14.7
CE	24.4	19.8	31.8	6.3
CE/TC	***0.71***	***0.27***	***0.64***	***0.43***

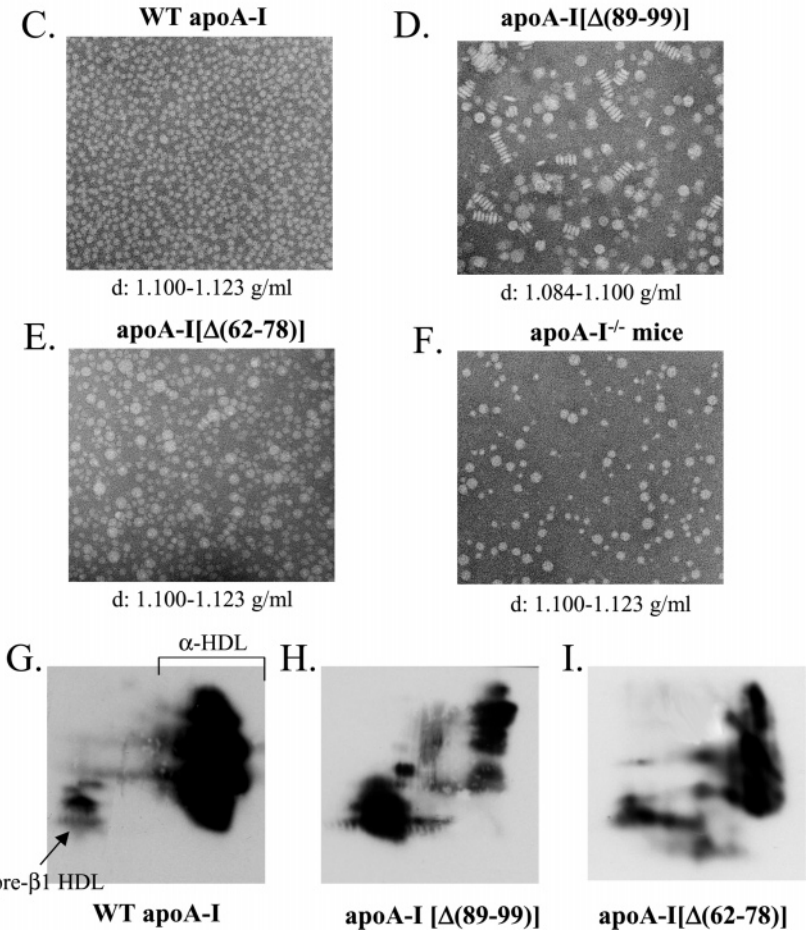

FIGURE 2: Analyses of plasma of apoA-I$^{-/-}$ mice expressing WT apoA-I or apoA-I[Δ(89−99)] and apoA-I[Δ(62−78)] mutants. **(**A)SDS−PAGE analysis of density gradient ultracentrifugation fractions of plasma of apoA-I$^{-/-}$ mice expressing WT or mutant apoA-I forms. Densities of the fractions are indicated at the top of the panel. (B) CE/TC ratio from a pool of lipoprotein fractions that correspond to the HDL region. (C−F) Electron microscopy pictures of HDL fractions obtained from apoA-I$^{-/-}$ mice expressing (C) WT apoA-I, (D) apoA-I[Δ(89−99)] mutant, and (E) apoA-I[Δ(62−78)] mutant or from control apoA-I$^{-/-}$ mice (F) following density gradient ultracentrifugation of plasma. Densities of the fractions used are indicated at the bottom of each picture. The photomicrographs were taken at 75000× magnification and enlarged 3 times. (G−I) Analysis of plasma obtained from mice expressing (G) WT apoA-I, (H) apoA-I[Δ(89−99)] mutant, and (I) apoA-I[Δ(62−78)] mutant following two-dimensional gel electrophoresis and Western blotting.

(ii) PLTP Activity Is Inhibited in the Plasma of Mice Expressing the ApoA-I[Δ(89−99)] Mutant. We analyzed the PLTP activity of plasma obtained from mice expressing WT apoA-I and the apoA-I[Δ(89−99)] and apoA-I[Δ(62−78)]

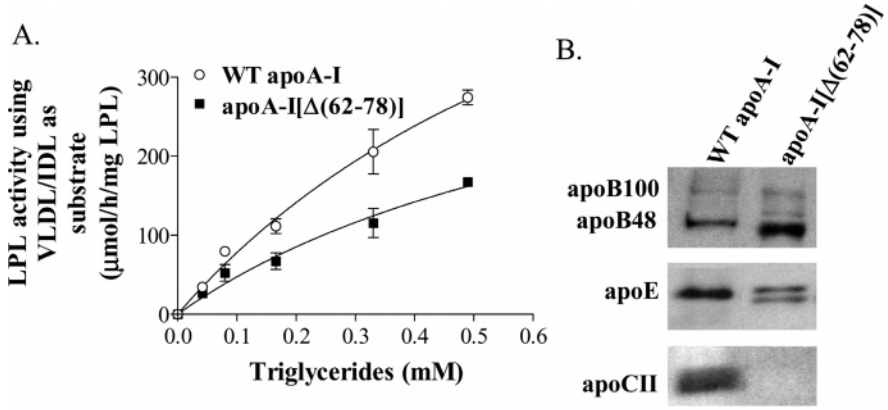

	Km_{app} (mM)	$Vmax_{app}$ (μmol/h/mg LPL)	$Vmax_{app}/Km_{app}$
WT apoA-I	0.87±0.28	753±171	869±118
apoA-I[Δ(62-78)]	0.80±0.22	426±79	531±95

d=1.022g/ml VLDL/IDL

FIGURE 3: Effect of WT apoA-I and apoA-I[Δ(62−78)] on the in vitro lipolysis and apolipoprotein composition of VLDL/IDL fraction. (A) Diagram of initial velocity of the hydrolysis of VLDL/IDL, obtained from mice expressing WT apoA-I and apoA-I[Δ(62−78)] mutant, versus the concentration of VLDL/IDL triglycerides. Kinetic parameters of the enzymatic reaction are shown at the bottom of the panel. (B) Apolipoprotein composition of VLDL/IDL of mice expressing WT apoA-I or apoA-I[Δ(62−78)] mutant.

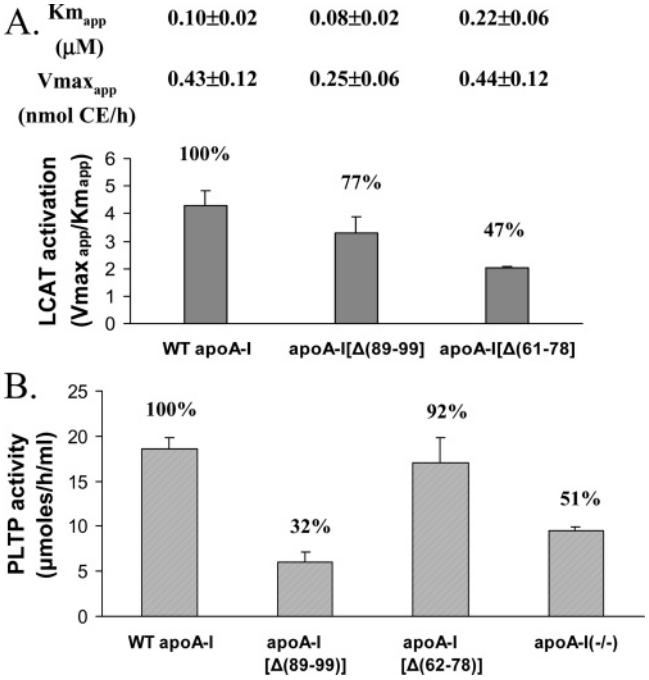

FIGURE 4: Functional analyses of WT and mutant apoA-I forms. (A) Activation of LCAT by rHDL containing WT or mutant apoA-I forms. The apparent K_m and V_{max} values and the catalytic efficiency V_{maxapp}/K_{mapp} of the enzyme are shown at the top of the panel. Values are the means ± SD from three independent experiments performed in duplicate. (B) PLTP activity in plasma obtained from apoA-I$^{-/-}$ mice infected with adenoviruses expressing WT apoA-I and apoA-I[Δ(89−99)] and apoA-I[Δ(62−78)] mutants and from apoA-I$^{-/-}$ mice infected with a control adenovirus expressing the GFP. Values are the means ± SD from four plasma samples assayed in duplicate.

mutants and apoA-I$^{-/-}$ mice infected with a control adenovirus expressing green fluorescence protein (GFP). This analysis showed that in mice expressing the apoA-I[Δ(89−99)] mutant the ability of PLTP to transfer phospholipids from multilamellar phospholipid particles to HDL was reduced to 32% of the WT control (Figure 4B). The apoA-I[Δ(62−78)] mutant showed a small reduction in PLTP activity that was not statistically significant. Reduced PLTP activity (51% of WT control) was also found in apoA-I$^{-/-}$ mice infected with a control adenovirus expressing GFP. The defective transfer of phospholipid may affect the maturation of the discoidal to spherical HDL particles and may be responsible for the accumulation of discoidal HDL in the plasma of mice expressing the apoA-I[Δ(89−99)] mutant.

The changes in the in vitro and in vivo parameters of the two apoA-I mutants are compiled in Table 2. Figure 5 is a schematic representation that indicates changes in the HDL biogenesis and catabolism that can account for the lipid and lipoprotein abnormalities observed in mice expressing the apoA-I[Δ(89−99)] mutant.

DISCUSSION

Adenovirus-mediated gene transfer offers a remarkable tool to study how structural alterations in apoA-I affect the biogenesis and functions of HDL, to ascertain the impact of apoA-I mutations on the overall plasma cholesterol and triglycerides homeostasis, and to correlate the observed in vivo phenotypes with known in vitro functions of apoA-I.

By screening the in vitro and in vivo properties of several apoA-I mutants (*2*, *6*, *7*), we were able to identify in the present study two mutations in the amino-terminal segment of apoA-I that have a profound effect on overall cholesterol and triglycerides homeostasis. Since apoA-I is essential for HDL biogenesis and catabolism, the expectation was that the apoA-I mutations would affect only the levels and/or the functions of HDL.

The first mutation has a deletion of residues 89−99 of apoA-I and produced an apoA-I phenotype that has not been encountered previously. Mice expressing this mutant have increased plasma cholesterol and phospholipids that accumulate in the VLDL/IDL/LDL region and form discoidal HDL particles.

Table 2: In Vivo Phenotypes of Mice Expressing the ApoA-I[Δ(89−99)] and ApoA-I[Δ(62−78)] Deletion Mutants and Changes in the in Vitro Functions of the Two ApoA-I Mutants

	in vivo phenotypes[a]						changes in in vitro functions[b]		
mutation	cholesterol (*x*-fold increase)	triglycerides (*x*-fold increase)	VLDL lipolysis	plasma PLTP activity (%)	EM particles	CE/TC (%)	activation of LCAT (%)	ABCA1-mediated cholesterol efflux (%)	SR-BI-mediated cholesterol efflux (%)
apoA-I[Δ(89−99)]	3.2	normal	decreased	32	discoidal	38[c]	77	68	78
apoA-I[Δ(62−78)]	2	9.5	ND[d]	92	spherical	90[c]	47	101	96

[a] Refers to parameters obtained from mice expressing apoA-I[Δ(89−99)] and apoA-I[Δ(62−78)] deletion mutants as compared to mice expressing WT apoA-I. [b] Refers to parameters determined by in vitro assays for the two apoA-I mutants as compared to the same parameters for the WT apoA-I. [c] Based on the data of Figure 2B. [d] ND, not determined.

FIGURE 5: Schematic representation of the defects in the HDL pathway that can account for the high plasma cholesterol levels and the discoidal HDL particles induced by the apoA-I[Δ(89−99)] mutant. PL, phospholipids; C, cholesterol.

It was shown previously that an apoA-I[Δ(88−98)] deletion mutant had approximately 50% LCAT activation capacity as compared to WT apoA-I (*18*). A more recent study showed that the apoA-I[Δ(88−98)] deletion mutant containing an amino-terminal His tag had greatly decreased α-helical content, reduced stability, reduced ability to activate LCAT in vitro, and defective dimyristoyl-L-α-phosphatidylcholine (DMPC) clearance (*19*). Similar analysis by us showed that the 89−99 deletion, which differs by two amino acids as compared to the 88−98 deletion, as well as the 61−78 deletion of apoA-I caused significant but less severe reduction in the α-helical content of the two mutant proteins as compared to the 88−98 deletion and resulted in lower cooperativity of thermal and chemical transition (I. N. Gorshkova, D. Atkinson, and V. I. Zannis, unpublished data). In our studies the deletion mutants apoA-I[Δ(89−99)] and apoA-[Δ(61−78)] did not contain a His tag that might have affected their physicochemical and functional properties.

In vitro analyses showed that apoA-I[Δ(89−99)] mutant that lacks the His tag had 77% capacity to activate LCAT compared to WT apoA-I. The LCAT activation capacity of apoA-I[Δ(89−99)] containing a His tag was reduced to 55% of the WT control. The observed differences in the physicochemical and functional properties between apoA-I[Δ(88−98)] and apoA-I[Δ(89−99)] may be related to the two amino acids difference of the two mutants as well as the presence of the His tag in the apoA-I[Δ(88−98)] mutant. As shown previously, the capacity of apoA-I[Δ(89−99)] to promote ABCA1-mediated cholesterol efflux was 68% (*7*). Finally, the capacity of this mutant to promote SR-BI-mediated cholesterol efflux was 78% (data not shown). Comparing the in vitro LCAT activation abilities of the apoA-I[Δ(89−99)] and apoA-I[Δ(61−78)] mutants (77% and 47% of the WT control), one would predict the apoA-I[Δ(89−99)] mutant would form spherical HDL particles. However, the animal experiments provide strong evidence that in vivo the activity of LCAT in mice expressing this mutant is seriously compromised. This is demonstrated by the increase in the preβ1 HDL and concomitant formation of discoidal HDL particles as well as the diminished esterification of the HDL and LDL cholesterol. Given the relatively high ABCA1-mediated cholesterol efflux promoted by this mutant in vitro, it is reasonable to assume that the 89−99 deletion did not affect grossly the ABCA1 lipidation of apoA-I. The combined data for the apoA-I[Δ(89−99)] and apoA-I[Δ(61−78)] mutants indicate that the in vitro catalytic efficiency (V_{maxapp}/K_{mapp}) of LCAT with rHDL particles as substrates may not be a good index of the in vivo catalytic activity of LCAT with its natural lipoprotein substrates. It is interesting that the CE/TC ratio of the HDL fraction derived from mice

expressing apoA-I[Δ(89−99)] is 38% of the WT control. In contrast, the CE/TC ratio of the HDL fraction derived from apoA-I$^{-/-}$ mice is 61% of the normal control.

The most exciting aspect of the apoA-I[Δ(89−99)] mutant, however, is its ability to affect cholesterol and phospholipid homeostasis by increasing their concentration in the VLDL/IDL and LDL region. To interpret these findings, we assayed the plasma activity of PLTP in mice infected with adenoviruses expressing WT apoA-I and apoA-I mutants. This analysis showed that the PLTP activity of mice expressing the apoA-I[Δ(89−99)] mutant was 32% as compared to the PLTP activity of the mice expressing the WT apoA-I. It has been proposed that PLTP functions by linking the donor and acceptor lipoprotein particles, thus facilitating the net transfer of phospholipids to HDL (*20*). Other studies showed that the PLTP activity could be retained on apoA-I affinity columns, indicating physical interactions between the two proteins (*21*). Monoclonal antibodies recognizing epitopes within the amino-terminal region, 27−141, of apoA-I prevented the binding of PLTP to apoA-I (*21*). PLTP was also shown to remodel the HDL and to promote the generation of preβ HDL particles (*22*−*24*). Studies are under way to map the domains and residues required for physical and functional interactions between apoA-I and PLTP. Deficiency of PLTP in mice decreased the HDL phospholipids and cholesterol levels on a chow or high-fat diet. On a high-fat diet, PLTP deficiency also increased the concentration of phospholipids and cholesterol in VLDL and LDL and promoted the formation of discoidal particles (*25*). The phenotype of the PLTP-deficient mice has remarkable similarities with the phenotype of mice expressing the apoA-I[Δ(89−99)] mutant. Taken together, these findings indicate that the observed reduction in PLTP activity by the apoA-I[Δ(89−99)] mutant may be physiologically significant. The PLTP activity was reduced in mice expressing apoA-I[Δ-(89−99)] but not in mice expressing apoA-I[Δ(62−78)] mutant. Diminished interactions between the apoA-I[Δ(89−99)] mutant and PLTP may inhibit the transfer of phospholipids from VLDL/IDL/LDL to HDL. The accumulation of phospholipids may cause a parallel increase in the cholesterol of VLDL/IDL/LDL fractions and thus induce hypercholesterolemia.

Figure 5 shows a putative pathway of biogenesis and catabolism of HDL that can explain the synthesis of discoidal HDL and the induction of hypercholesterolemia in mice expressing the apoA-I[Δ(89−99)] mutant.

The second mutation has a deletion of residues 62−78 of apoA-I and caused combined hyperlipidemia, characterized by high plasma cholesterol and severe hypertriglyceridemia. This phenotype has been also observed in mice expressing an apoA-I mutant where Glu110 and Glu111 have been mutated to Ala (*8*).

It is interesting that a previous study suggested that lipid-free WT apoA-I binds to the high-affinity HDL receptor for apoA-I, β-chain of ATP synthase, and that peptides corresponding to the 62−77 region of apoA-I identified this sequence as a high-affinity ligand domain for this receptor (*26*−*28*). However, the correlation of this property of apoA-I with the observed dyslipidemia is not obvious.

A series of assays were performed in vitro in order to correlate the in vitro parameters with the observed in vivo phenotype. These analyses showed that the apoA-I[Δ(61−78)] mutant had normal capacity to promote ABCA1-mediated cholesterol efflux (*7*) and SR-BI-mediated cholesterol efflux (data not shown), but its capacity to activate LCAT was 47% of the WT control. Nevertheless, these levels of LCAT activation by this apoA-I mutant were sufficient to promote formation of spherical αHDL particles in vivo, as determined by EM analysis. Furthermore the CE/TC ratio of the HDL fraction derived from mice expressing apoA-I[Δ(62−78)] is 90% of the normal control. This mutant did not affect the plasma activity of PLTP. The findings indicate that the apoA-I[Δ(62−78)] mutant, which is associated with hypertriglyceridemia, is not defective in the formation and maturation of HDL.

Density gradient ultracentrifugation of plasma showed that the VLDL/IDL fraction obtained from mice expressing the apoA-I[Δ(62−78)] mutant contains apoA-I. The rate of in vitro lipolysis of this fraction was 61% of the lipolysis of the VLDL/IDL fraction obtained from mice expressing WT apoA-I. In addition, in vitro experiments also showed that addition of ∼60 μg/mL of either WT or mutant apoA-I to triglycerides emulsions inhibits their lipolysis by LPL by 40% (data not shown). Finally, the VLDL/IDL fraction of mice expressing the apoA-I[Δ(62−78)] mutant had greatly diminished levels of apoCII and increased levels of apoB48. Taken together, these findings are consistent with diminished in vivo lipolysis of VLDL/IDL remnants in mice expressing the apoA-I[Δ(62−78)] mutant.

The molecular etiology of common forms of combined hyperlipidemia characterized by high plasma cholesterol and triglycerides as well as hypercholesterolemia remains unknown. The present study points to the possibility that subtle changes in the structure of apoA-I may underlie conditions of dyslipidemia in humans similar to those observed in mice expressing the mutant apoA-I forms described in this study. It also indicates that apoA-I and HDL may play a crucial but still unidentified role in plasma cholesterol and triglycerides homeostasis. The dyslipidemia induced by apoA-I mutations may be further aggravated by other genetic and environment factors in humans such as diabetes, thyroid status, etc. The potential role of apoA-I mutations in dyslipidemia will be addressed in the future by studies in transgenic mice, as well as in selected populations of dyslipidemic patients that may harbor mutations in apoA-I.

ACKNOWLEDGMENT

We thank Dr. Silvia Santamarina-Fojo for providing the LCAT adenovirus and Ms. Gayle Forbes for technical assistance.

REFERENCES

1. Zannis, V. I., Kardassis, D., and Zanni, E. E. (1993) Genetic mutations affecting human lipoproteins, their receptors, and their enzymes, *Adv. Hum. Genet. 21*, 145−319.
2. Chroni, A., Liu, T., Gorshkova, I., Kan, H. Y., Uehara, Y., von Eckardstein, A., and Zannis, V. I. (2003) The central helices of apoA-I can promote ATP-binding cassette transporter A1 (ABCA1)-mediated lipid efflux. Amino acid residues 220−231 of the wild-type apoA-I are required for lipid efflux in vitro and high-density lipoprotein formation in vivo, *J. Biol. Chem. 278*, 6719−6730.
3. Laccotripe, M., Makrides, S. C., Jonas, A., and Zannis, V. I. (1997) The carboxyl-terminal hydrophobic residues of apolipoprotein A-I affect its rate of phospholipid binding and its association with high-density lipoprotein, *J. Biol. Chem. 272*, 17511−17522.

4. Liu, T., Krieger, M., Kan, H. Y., and Zannis, V. I. (2002) The effects of mutations in helices 4 and 6 of apoA-I on scavenger receptor class B type I (SR-BI)-mediated cholesterol efflux suggest that formation of a productive complex between reconstituted high-density lipoprotein and SR-BI is required for efficient lipid transport, *J. Biol. Chem. 277*, 21576−21584.
5. Zannis, V. I., Chroni, A., Kypreos, K. E., Kan, H. Y., Cesar, T. B., Zanni, E. E., and Kardassis, D. (2004) Probing the pathways of chylomicron and HDL metabolism using adenovirus-mediated gene transfer, *Curr. Opin. Lipidol. 15*, 151−166.
6. Reardon, C. A., Kan, H. Y., Cabana, V., Blachowicz, L., Lukens, J. R., Wu, Q., Liadaki, K., Getz, G. S., and Zannis, V. I. (2001) In vivo studies of HDL assembly and metabolism using adenovirus-mediated transfer of ApoA-I mutants in ApoA-I-deficient mice, *Biochemistry 40*, 13670−13680.
7. Chroni, A., Liu, T., Fitzgerald, M. L., Freeman, M. W., and Zannis, V. I. (2004) Cross-linking and lipid efflux properties of apoA-I mutants suggest direct association between apoA-I helices and ABCA1, *Biochemistry 43*, 2126−2139.
8. Chroni, A., Kan, H. Y., Kypreos, K. E., Gorshkova, I. N., Shkodrani, A., and Zannis, V. I. (2004) Substitutions of glutamate 110 and 111 in the middle helix 4 of human apolipoprotein A-I (apoA-I) by alanine affect the structure and in vitro functions of apoA-I and induce severe hypertriglyceridemia in apoA-I-deficient mice, *Biochemistry 43*, 10442−10457.
9. Williamson, R., Lee, D., Hagaman, J., and Maeda, N. (1992) Marked reduction of high density lipoprotein cholesterol in mice genetically modified to lack apolipoprotein A-I, *Proc. Natl. Acad. Sci. U.S.A. 89*, 7134−7138.
10. Fielding, C. J., and Fielding, P. E. (1996) Two-dimensional nondenaturing electrophoresis of lipoproteins: applications to high-density lipoprotein speciation, *Methods Enzymol. 263*, 251−259.
11. Damen, J., Regts, J., and Scherphof, G. (1982) Transfer of [^{14}C]-phosphatidylcholine between liposomes and human plasma high-density lipoprotein. Partial purification of a transfer-stimulating plasma factor using a rapid transfer assay, *Biochim. Biophys. Acta 712*, 444−452.
12. Speijer, H., Groener, J. E., van Ramshorst, E., and van Tol, A. (1991) Different locations of cholesteryl ester transfer protein and phospholipid transfer protein activities in plasma, *Atherosclerosis 90*, 159−168.
13. Hill, J. S., Wang, X., Paranjape, S., Dimitrijevich, D., Lacko, A. G., and Pritchard, P. H. (1993) Expression and characterization of recombinant human lecithin:cholesterol acyltransferase, *J. Lipid Res. 34*, 1245−1251.
14. Jin, L., Lee, Y. P., and Jonas, A. (1997) Biochemical and biophysical characterization of human recombinant lecithin: cholesterol acyltransferase, *J. Lipid Res. 38*, 1085−1093.
15. Amar, M. J. A., Shamburek, R. D., Foger, B., Hoyt, R. F., Wood, D. O., Santamarina-Fojo, S., and Brewer, H. B. (1998) Adenovirus-mediated expression of LCAT in nonhuman primates leads to an antiatherogenic lipoprotein profile with increased HDL and decreased LDL, *Circulation Suppl. 98*, I-35.
16. Matz, C. E., and Jonas, A. (1982) Micellar complexes of human apolipoprotein A-I with phosphatidylcholines and cholesterol prepared from cholate−lipid dispersions, *J. Biol. Chem. 257*, 4535−4540.
17. Kypreos, K. E., Van Dijk, K. W., van Der, Z. A., Havekes, L. M., and Zannis, V. I. (2001) Domains of apolipoprotein E contributing to triglyceride and cholesterol homeostasis in vivo. Carboxyl-terminal region 203−299 promotes hepatic very low-density lipoprotein-triglyceride secretion, *J. Biol. Chem. 276*, 19778−19786.
18. Sorci-Thomas, M., Kearns, M. W., and Lee, J. P. (1993) Apolipoprotein A-I domains involved in lecithin-cholesterol acyltransferase activation. Structure:function relationships. *J. Biol. Chem. 268*, 21403−21409.
19. Rogers, D. P., Roberts, L. M., Lebowitz, J., Datta, G., Anantharamaiah, G. M., Engler, J. A., and Brouillette, C. G. (1998) The lipid-free structure of apolipoprotein A-I: effects of amino-terminal deletions, *Biochemistry 37*, 11714−11725.
20. Huuskonen, J., Olkkonen, V. M., Jauhiainen, M., and Ehnholm, C. (2001) The impact of phospholipid transfer protein (PLTP) on HDL metabolism, *Atherosclerosis 155*, 269−281.
21. Pussinen, P. J., Jauhiainen, M., Metso, J., Pyle, L. E., Marcel, Y. L., Fidge, N. H., and Ehnholm, C. (1998) Binding of phospholipid transfer protein (PLTP) to apolipoproteins A-I and A-II: location of a PLTP binding domain in the amino terminal region of apoA-I, *J. Lipid Res. 39*, 152−161.
22. Jauhiainen, M., Metso, J., Pahlman, R., Blomqvist, S., van Tol, A., and Ehnholm, C. (1993) Human plasma phospholipid transfer protein causes high-density lipoprotein conversion, *J. Biol. Chem. 268*, 4032−4036.
23. Tu, A. Y., Nishida, H. I., and Nishida, T. (1993) High-density lipoprotein conversion mediated by human plasma phospholipid transfer protein, *J. Biol. Chem. 268*, 23098−23105.
24. von Eckardstein, A., Jauhiainen, M., Huang, Y., Metso, J., Langer, C., Pussinen, P., Wu, S., Ehnholm, C., and Assmann, G. (1996) Phospholipid transfer protein mediated conversion of high-density lipoproteins generates pre beta 1-HDL, *Biochim. Biophys. Acta 1301*, 255−262.
25. Jiang, X. C., Bruce, C., Mar, J., Lin, M., Ji, Y., Francone, O. L., and Tall, A. R. (1999) Targeted mutation of plasma phospholipid transfer protein gene markedly reduces high-density lipoprotein levels, *J. Clin. Invest 103*, 907−914.
26. Barbaras, R., Collet, X., Chap, H., and Perret, B. (1994) Specific binding of free apolipoprotein A-I to a high-affinity binding site on HepG2 cells: characterization of two high-density lipoprotein sites, *Biochemistry 33*, 2335−2340.
27. Georgeaud, V., Garcia, A., Cachot, D., Rolland, C., Terce, F., Chap, H., Collet, X., Perret, B., and Barbaras, R. (2000) Identification of an ApoA-I ligand domain that interacts with high-affinity binding sites on HepG2 cells, *Biochem Biophys Res. Commun. 267*, 541−545.
28. Martinez, L. O., Jacquet, S., Esteve, J. P., Rolland, C., Cabezon, E., Champagne, E., Pineau, T., Georgeaud, V., Walker, J. E., Terce, F., Collet, X., Perret, B., and Barbaras, R. (2003) Ectopic beta-chain of ATP synthase is an apolipoprotein A-I receptor in hepatic HDL endocytosis, *Nature 421*, 75−79.

BI047998L